 doi:10.20944/preprints202205.0013.v1

On sound scattering and acoustic properties of the upper layer of the sea with bubble clouds

V.A. Bulanov, L.K. Bugaeva, A.V. Storozhenko

V.I. Ilyichev Pacific Oceanological Institute, Far East Branch of Russian Academy of Sciences, Vladivostok, Russia, bulanov@poi.dvo.ru

Keywords: sea water, bubbles, plankton, sound scattering, sound attenuation, acoustic spectroscopy

Abstract

The presence of bubbles near the sea surface under certain conditions leads to abnormal sound scattering and a significant change in the acoustic properties of the upper layer of the sea. The article presents some results of sound scattering studies under various sea conditions, up to stormy conditions, when extensive bubble clouds arise. By the method of unsteady acoustic spectroscopy, data on the size distribution of bubbles at various depths have been obtained, which can be described by a power function with exponential decay at small bubble sizes of the order of 10 microns. Estimates of the gas content in bubble clouds and their influence on the acoustic characteristics of the upper layer of the sea have been carried out. It is shown that at sufficiently high concentrations, sharp increases in absorption and dispersion of the sound velocity are observed. Modeling of sound propagation in the presence of a quasi-homogeneous bubble layer shows that it leads both to a change in the laws of the average decay of the sound field along the sound propagation path and to a change in the shallow spatial structure of the field.

Introduction

According to its hydrophysical characteristics, the upper layer of the sea sharply differs from the rest of the marine environment. The near-surface layer of the ocean water column changes significantly with strong winds and developed surface waves [1-9]. Under these conditions, it is characterized by developed turbulence, abnormally high concentrations of gas bubbles, gas saturation of water and a large gas exchange between the ocean and the atmosphere. [3-7, 9-13]. Under these conditions, acoustic characteristics also change, such as the coefficients of scattering, absorption and dispersion of the speed of sound, the parameter of the nonlinearity of seawater, which become dependent on the presence of air bubbles formed when wind waves collapse [1-3, 6-8, 14-16]. Along with the change in these average characteristics of the near-surface layer, their fluctuations are sharply pronounced, which are associated with bubble structures that are born when wind waves collapse [4, 5-8]. These structures, as a rule, affect the scattering and propagation of sound [14-16].

The aim of the work is to study the structure and dynamic characteristics of the upper layer of the sea saturated with gas bubbles, as well as the relationship between the acoustic characteristics

Preprints (www.preprints.org) | NOT PEER-REVIEWED | Posted: 4 May 2022 doi:10.20944/preprints202205.0013.v1

of the agitated upper layer of the sea and the characteristics of bubble clouds formed by the collapse of surface waves in strong winds.

The measurement of the concentration of bubbles and their size distribution g(R) in the sea was carried out by various methods (mainly optical and acoustic) and the results are presented in a large number of papers [1-14]. Nevertheless, many issues of the distribution of bubbles in depth and the regularities of the evolution of the g(R) function over time after the passage of various disturbances, including the effects of the collapse of wind waves and their relaxation to an undisturbed state, remained unclear [10-13]. It is usually assumed that bubble clouds arise after the collapse of surface waves in local regions of space and such clouds are distributed quite freely, so that the characteristic horizontal size of the cloud is less than the distance between neighboring clouds. However, at sufficiently high wind speeds, during the transition to stormy conditions, the distance between local clouds is reduced, the saturation of the upper layer with gas increases sharply and at the same time the lifetime of local bubble clouds increases, which often leads to the overlap of individual clouds and the formation of a continuous bubble layer inhomogeneous in space. The acoustic properties of such a layer remain poorly studied in many respects. One of the main problems in measuring the characteristics of the bubble layer under various meteorological conditions is the need to carry out long-term measurements with high spatial and temporal resolution [5,6]. Such measurements in shallow seas can be carried out using radiators installed on the bottom and directed vertically upwards. To implement such measurements, a set of emitters with different radiation frequencies is usually used in order to maximize the overlap of the spectral region of bubble structures. As a rule, narrow-beam linear acoustic emitters are used to locate clouds. There is also experience in the use of parametric acoustic emitters that allow scanning in the range of difference frequencies with a little varying pumping frequency and maintaining the directional characteristics in a wide range of difference frequencies [17,18]. An important problem is the separation of scattering on resonant bubbles from scattering on non-resonant bubbles and other heterogeneous and homogeneous inhomogeneities of the water column (plankton, suspensions, turbulence). The use of unsteady scattering [17, 18] of sharply directed ultrasound beams using parametric acoustic emitters makes it possible to separate resonant scattering from the non-resonant background and obtain experimental data on the structure of bubble clouds formed when wind waves collapse and their involvement in the sea thickness. The main objective of this work was to study the distribution of scattering coefficients, absorption and dispersion of the sound velocity of seawater in the near-surface layer of the sea in relation to the distribution of bubbles in the upper layer of the sea.

2. Materials and Methods

2.1. Theoretical foundations

The basis of the method for measuring the size distribution of g(R) in the sea is based on sound scattering measurements [1-3, 5,6]. The study of the backscattering of acoustic pulses in clouds of bubbles in a shallow sea often occurs with the use of inverted radiators installed on the bottom of the sea. Having information about the amplitudes of the V wave incident on the volume and scattered in the opposite direction, it is possible to determine the volume scattering coefficient in the form of [1] in the single scattering approximation (Born approximation):

$$m_V = \frac{2}{\pi\theta^2 c\tau}\left(\frac{P_{bs}}{P_i}\right)^2, \qquad P_i(r) = A\frac{e^{-\alpha r}}{r}, \tag{1}$$

where θ is the width of the emitter directivity characteristic, c is the speed of sound, τ is the duration of the sound pulse, α is the sound absorption coefficient when the sound absorption at

Preprints (www.preprints.org) | NOT PEER-REVIEWED | Posted: 4 May 2022 doi:10.20944/preprints202205.0013.v1

a distance r is small, $P_i(r) \approx A/r$, A is the calibration value of the amplitude of the emitted sound, measured in pascals and usually reduced to a distance of 1 meter.

The value P_{bs} is measured directly in the experiment. Using the repeated use of pulses, it is possible using formula (1) to register the change in time of the average scattering coefficient of sound and its fluctuations in the entire thickness of the liquid with a high spatial resolution determined by the width of the directional characteristic of the emitter θ and the length of the acoustic pulse $l_{imp} = c\tau/2$, and a high temporal resolution determined by the time interval between the pulses of the emitted sound. If the calibration for the coefficient A in formula (1) is missing or has changed, its value can be restored based on the available information on sound reflection from the media interface. The main step is to determine the value of A in ideal conditions of a calm sea without waves and near-surface bubbles. Under these conditions, we can put that $\alpha h << 1$ and $V \approx -1$. If we measure the pressure in the first reflected pulse, we can find the value A in the form $A = P_h 2h$. Then $P_i(r) = P_h \exp(-\alpha r)(2h/r) \approx P_h(2h/r)$ and we finally get

$$m_V(r) = \frac{1}{2\pi c\tau\theta^2}\left(\frac{P_{bs}(r)}{P_h}\right)^2\left(\frac{r}{h}\right)^2 \exp\left(\int_0^r \alpha(x)dx\right). \quad (2)$$

Differentiating (2) by r, one can obtain an equation relating the sound absorption and the scattering coefficient

$$\alpha(r) = d/dr\left\{\ln\left[m_V(r)\Big/\left(r^2 P_{bs}(r)^2\right)\right]\right\}. \quad (3)$$

The simplest bubble size distribution function $g(R)$ can be found by the frequency dependence of the sound scattering coefficient $m_V(\omega)$, assuming that the main contribution to sound scattering is made by resonant bubbles whose radius $R(\omega)$ is related to the frequency ω according to the Minnert formula [2, 3, 6]:

$$g(R(\omega)) = \frac{2\delta_\omega}{\pi R^3(\omega)} m_V(\omega), \qquad R(\omega) = \sqrt{3\gamma P_0/\rho}\Big/\omega, \quad (4)$$

where δ_ω is the coefficient of resonant attenuation on frequency ω, P_0 is hydrostatic pressure, $\gamma \approx 1.4$ is adiabatic constant of the gas inside the bubble, ρ is a density of the liquid.

In the presence of other non-resonant inclusions along with resonant bubbles , the total sound scattering coefficient from the unit volume of the medium m_V can be written as [17, 18]:

$$m_V = m_V^{(b)} + m_V^{(s)} = \int_{\{R\}}\left[\left|f^{(b)}\right|^2 g^{(b)}(R) + \left|f^{(s)}\right|^2 g^{(s)}(R)\right]dR. \quad (5)$$

Here, $f^{(b)}$ and $f^{(s)}$ are the amplitudes of monopole (volumetric) stationary sound scattering on bubbles and non-resonant inclusions, indices (b) and (s) indicate that the quantities belong to bubbles. and non-resonant inclusions, respectively. Note that the function $g(R)$ is related to the number of bubbles per unit volume by the formula $N = \int_{R_{\min}}^{R_{\max}} g(R)dR$. The expression for $f^{(b)}$ has the following form [1-3, 6]

$$f^{(b)} = R\Big/\left\{\left[\left(R_\omega^2/R^2\right)-1\right]^2 + \delta_\omega^2\right\}. \quad (6)$$

Taking into account transients when the bubble is swinging at resonance leads to a dependence of $m_V^{(b)}$ on the pulse duration τ [18]:

Preprints (www.preprints.org) | NOT PEER-REVIEWED | Posted: 4 May 2022 doi:10.20944/preprints202205.0013.v1

$$m_V^{(b)}(\tau) = m_V^{(b)}(\infty) F(\tau/\tau_0), \qquad m_V^{(b)}(\infty) = (\pi/2) R^3 g^{(b)}(R)/\delta(R) \tag{7}$$

$$F(\tau/\tau_0) = 1 - \left[1 - \exp(\tau/\tau_0)\right]/(\tau/\tau_0), \qquad \tau_0 = 1/\omega\delta = Q/\omega. \tag{8}$$

Here $m_V^{(b)}(\infty)$ is the coefficient of stationary resonant scattering on bubbles. The function $F(\tau/\tau_0)$ determines the evolution of the cross-section of the non-stationary resonant scattering, therefore it helps in practice to separate the resonant scattering from the non-resonant background, as well as to determine the Q-factor of bubbles at different frequencies according to the formula (8). The use of frequency-tunable directional emitters makes it possible to implement non-stationary acoustic spectroscopy of bubbles [18] in the form:

$$W^2(\tau) = (\pi c\theta^2/2)\left[m_V^{(b)}(\tau) + m_V^{(s)}\right], \qquad W(\tau) = \left(1/\sqrt{\tau}\right)(P_s/P_i), \tag{9}$$

$$g^{(b)}(R) = 4\delta(R)\left[W^2(\infty) - W^2(0)\right]/\left(\pi^2 c\theta^2 R^3\right). \tag{10}$$

The scattering coefficient on the remaining inclusions can be determined by the formula:

$$m_V^{(s)} = 2W^2(0)/\left(\pi^2 c\theta^2 R^3\right). \tag{11}$$

The designations $W(\infty)$ and $W(0)$ correspond to the conditions $\tau >> \tau_0$ and $\tau << \tau_0$, respectively. Thus, the bubble size distribution function can be determined from the data of the inverse linear scattering of acoustic pulses of long and short duration.

2.2. Evaluation of acoustic characteristics based on a homogeneous model of water with bubbles

To describe the acoustic properties of a micro-homogeneous fluid, effective acoustic parameters are often used, which are usually determined within the framework of a homogeneous continuum model [1, 7, 15, 19]. The effective density of a micro-homogeneous liquid can be determined using the equations

$$\rho_e = \rho(1-x) + \rho' x, \qquad x = \frac{4}{3}\pi \int_{R_{\min}}^{R_{\max}} R^3 g(R) dR, \tag{12}$$

where ρ and ρ' is the density of the liquid and the contents of the bubble, respectively, the strokes hereafter refer to bubbles. The effective compressibility of a micro-homogeneous liquid, defined as $\beta_e = (1/\rho_e)(d\rho_e/dP) \equiv (\rho_e)_P/\rho_e$, is equal to [19,20]

$$\beta_e = \beta + \frac{4}{3}\pi \int_{R_{\min}}^{R_{\max}} (K - \beta) R^3 g(R) dR \equiv \beta + x(K - \beta). \tag{13}$$

Taking into account the polydispersity of the bubble mixture in general, the designations $x(K-\beta)$ hereafter should be understood in an integral sense, as a result of the effect of the integral operator x on the function $(K-\beta)$, leading to an expression $(4\pi/3)\int_{R_{\min}}^{R_{\max}} (K-\beta) R^3 g(R) dR$ that takes into account the size distribution of bubbles. With a monodisperse distribution $g(R) \square \delta(R - \bar{R})$, the value x is the usual volume concentration $x = (4\pi/3)\bar{R}^3 N$, where N is the number of bubbles of the same radius $\bar{R}$ per unit volume of the liquid. There is the following relation between $g(R)$ and the concentration of bubbles per unit volume $N = \int_{R_{\min}}^{R_{\max}} g(R) dR$, where $g(R) = dN/dR$. The compressibility of a single bubble in a liquid K takes into account the resonant and relaxation responses of bubbles to the influence of an external force and, in general, the value K is a complex function of the size of the bubble and the frequency of sound $K \equiv K(R, \omega)$ [18-20]. In the absence of these effects, the

Preprints (www.preprints.org) | NOT PEER-REVIEWED | Posted: 4 May 2022 doi:10.20944/preprints202205.0013.v1

compressibility K is equal to the compressibility of the material of a single bubble, i.e. $K \equiv \beta'$. In this case, the effective velocity of sound in a liquid with bubbles $\tilde{c}_e$ can be calculated based on a generalization of Wood's formula [19, 20]

$$\tilde{c}_e = \frac{1}{\sqrt{(\rho_e)_P}} = \frac{1}{\sqrt{\rho_e \beta_e}}, \tag{14}$$

which formally looks like the well-known Wood formula, but with modified effective parameters ρ_e and β_e in accordance with (12) and (13). The real part $c_e = \mathrm{Re}(\tilde{c}_e)$ determines the phase velocity of the pressure wave in the form:

$$c_e = c\,\mathrm{Re}\left\{\left[1+\frac{4}{3}\pi\int_{R_{\min}}^{R_{\max}}\left(\frac{K-\beta}{\beta}\right)R^3 g(R)dR\right]\left[1-x\right]\right\}^{-1/2}. \tag{15}$$

The attenuation coefficient α of a wave propagating in a liquid with bubbles can be determined using the wave number $\alpha = \mathrm{Im}\,k_e = \omega\,\mathrm{Im}(1/\tilde{c}_e)$ and formula (3) in the form:

$$\alpha = \mathrm{Im}(k_e) = (\omega/c)\,\mathrm{Im}\left[1+\frac{4}{3}\pi\int_{R_{\min}}^{R_{\max}}\left(\frac{K-\beta}{\beta}\right)R^3 g(R)dR\right]^{1/2}. \tag{16}$$

Taking into account the resonant properties of bubble compressibility $K \equiv K(R,\omega)$, the effective sound velocity c_e and sound absorption coefficient α can be calculated using formulas (15), (16) with parameters obtained using experimental data at low concentrations x:

$$c_e \approx c\,\mathrm{Re}\left(1-\frac{2\pi}{3}\frac{\rho c^2}{\gamma P_0}\int_0^\infty \frac{g(R)dR}{q(R,R_\omega)}\right), \tag{17}$$

$$\alpha \approx \frac{\omega}{c}\,\mathrm{Im}\left(\frac{2\pi}{3}\frac{\rho c^2}{\gamma P_0}\int_0^\infty \frac{g(R)dR}{q(R,R_\omega)}\right), \tag{18}$$

where $q(R,R_\omega) = 1-(R/R_\omega)^2(1+i/Q_\omega)$, $Q_\omega = 1/\delta_\omega$ is the Q-factor of a bubble of radius R_ω.

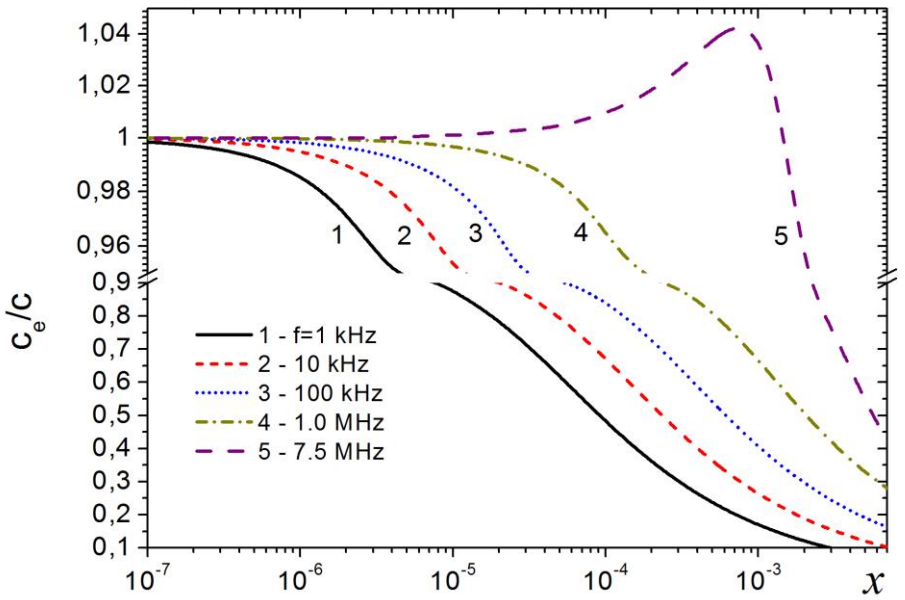

Fig. 1. The dependence of the speed of sound in water with a polydisperse mixture of bubbles on the concentration at different frequencies: 1 kHz (1), 10 kHz (2), 100 kHz (3), 1 MHz (4), 7.5 MHz (5).

Preprints (www.preprints.org) | NOT PEER-REVIEWED | Posted: 4 May 2022 doi:10.20944/preprints202205.0013.v1

Figure 1 shows the concentration dependence of the dimensionless sound velocity of water with gas bubbles $c_e(x)/c$ at $T = 20^0 C$, calculated for different sound frequencies in the case of a polydisperse mixture of bubbles for a power function of the bubble size distribution $g(R) = A_g R^{-n}$ at n=3.8 in the size range from R_{min} =0.1 mkm to R_{max} =2000 mkm. Figure 1 shows that in the concentration range x from 10^{-6} to 10^{-5} there is a sharp decrease in the speed of sound in a liquid with bubbles.

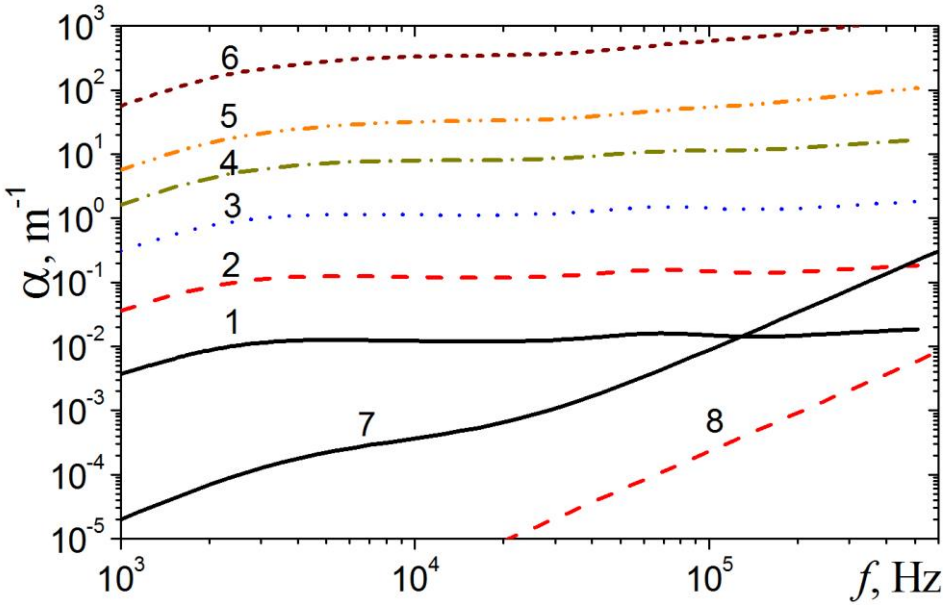

Fig. 2. Frequency dependence of the sound absorption coefficient in water at a temperature of 20^0 C with a polydisperse mixture of bubbles at different gas concentrations in the bubbles x: 1 – x=10^{-8}, 2 – 10^{-7}, 3 – 10^{-6}, 4 – 10^{-5}, 5 – 10^{-4}, 6 – 10^{-2}, 7 – x=0, sea water, 8 – x=0, fresh water

In Fig. 2 shows the frequency dependence of the sound absorption coefficient α in water with bubbles at T=20^0C, calculated by formula (18) for a polydisperse mixture of bubbles at different volume concentrations of gas in bubbles $x = (4\pi/3)\int_0^\infty R^3 g(R) dR$, taking into account formula (12). Here is also the frequency dependence of the sound absorption coefficient in fresh water $\alpha_0(f)$ and seawater $\alpha_{sea}(f)$ at T=20^0C and salinity 35 ppm. The frequency dependence of the sound absorption coefficient in fresh water $\alpha_0(f) \approx 2.3 \cdot 10^{-14} f^2$ (where α is in 1/m, f is in Hz) and the frequency dependence of the sound absorption coefficient in seawater according to the Sheehy-Halle formula [1]. It can be seen that in water with bubbles, the frequency dependence $\alpha(f)$ is weakly expressed. Such a weak frequency dependence is associated with the well-known predominant mechanism of resonant attenuation in a veil of bubbles with a wide bubble size distribution function $g(R)$ [1]. It should be noted that at high frequencies with small concentrations of bubbles less than x_b~10^{-8}, the contribution to sound absorption in pure seawater without bubbles may prevail over the contribution from bubbles. In fresh water, the specified threshold x_b is reduced by an order of magnitude. At concentrations of bubbles in the near-surface layers of seawater x~10^{-6} - 10^{-5} in conditions of developed excitement, the attenuation of sound will be entirely determined by the structure of the bubble cloud.

Preprints (www.preprints.org) | NOT PEER-REVIEWED | Posted: 4 May 2022 doi:10.20944/preprints202205.0013.v1

2.3. Experimental methods and equipment

Experimental work was carried out in the shallow sea. In Vityaz Bay of the Sea of Japan (100 km south of Vladivostok), a bottom system with sonar emitting and receiving antennas (depth of 12 meters) was installed for the purpose of long-term study of acoustic characteristics in the sea under various hydrometeorological conditions (Fig.1).

The acoustic system for measuring sound scattering included a sound emission path with different frequencies, piezoceramic converters, a reception path and a system for input and primary processing of acoustic information. The system of input and primary processing of acoustic information included a 14-bit interface input board of the company "Rudnev and Shilyaev" La2-USB with a maximum quantization frequency of 400 kHz, an interface 12-bit input board of the company "L-Card" E20-10 with a maximum quantization frequency of 10 MHz, personal computers and special programs processing and visualization of acoustic signals.

One of the important components of the system was a three–element emitter having the width of the main lobe of the directivity characteristic at a frequency of 138 kHz equal to 11.5^0, at a frequency of 216 kHz is 7.2^0, at a frequency of 519 kHz is 3^0. In addition, a non-directional broadband hydrophone is installed for recording, calibrating and monitoring radiation. As a parametric emitter at pumping frequencies of 200 kHz at difference frequencies of 15-40 kHz, the FURUNO emitter type CA200-8B (Japan) was most often used, with an operating frequency of 200 kHz and a maximum permissible power of 2 kW. The width of the radiation pattern at the operating frequency is 5.6^0.

The coastal equipment allowed for multi-frequency measurement of scattering signals by various methods. The method of simultaneous emission of pulses of different frequencies was used, followed by filtering of the received signals through channels [21] (Fig.1).

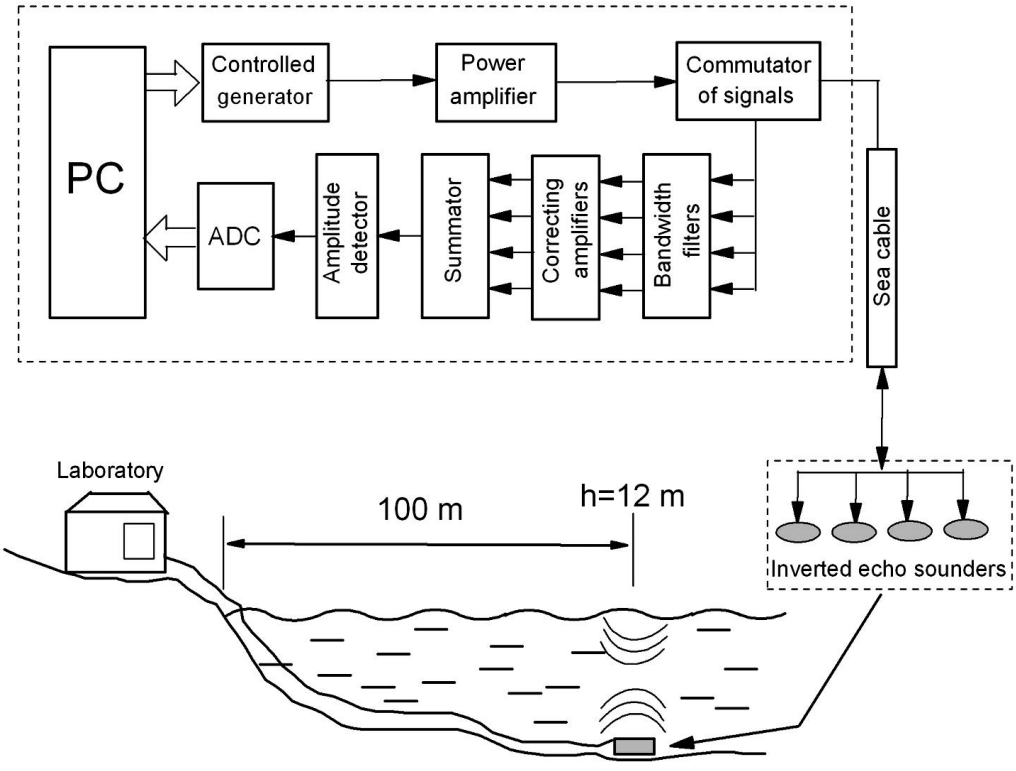

Fig. 3. The scheme of acoustic measurements from the bottom station.

Preprints (www.preprints.org) | NOT PEER-REVIEWED | Posted: 4 May 2022 doi:10.20944/preprints202205.0013.v1

The programmable generator GSPF-053 of the company "Rudnev and Shilyaev" (Moscow) was used as a digital signal generator. Broadband power amplifiers of the U7-5 type were used as pre-amplifiers. Terminal amplifiers were amplifiers made on the basis of high-voltage transistors and allowed to raise the output voltage to 400 volts. The signal switch was made according to the scheme of diode switches of echo sounders. For narrowband filtering and amplification, selective nanovoltmeters SN-233 and SN-232 from UNIPAN (Poland), third-octave filters RFT01018 from Robotron (Germany), microphone amplifiers RFT00011 from Robotron (Germany), filters for individual frequencies were manufactured in the laboratory of hydrophysics of the POI FEB RAS. The coastal equipment was located in the immediate vicinity of the bottom station and was connected by an underwater cable (Fig.1).

3. Results

3.1. Sound scattering in the near-surface layer of the sea

A typical distribution of the volume scattering coefficient of sound $m_V(z,t)$ obtained using the bottom system is shown in Fig. 4. The tidal fluctuations of the sea level are clearly visible in Fig. 4. The night period is marked in gray on the time axis.

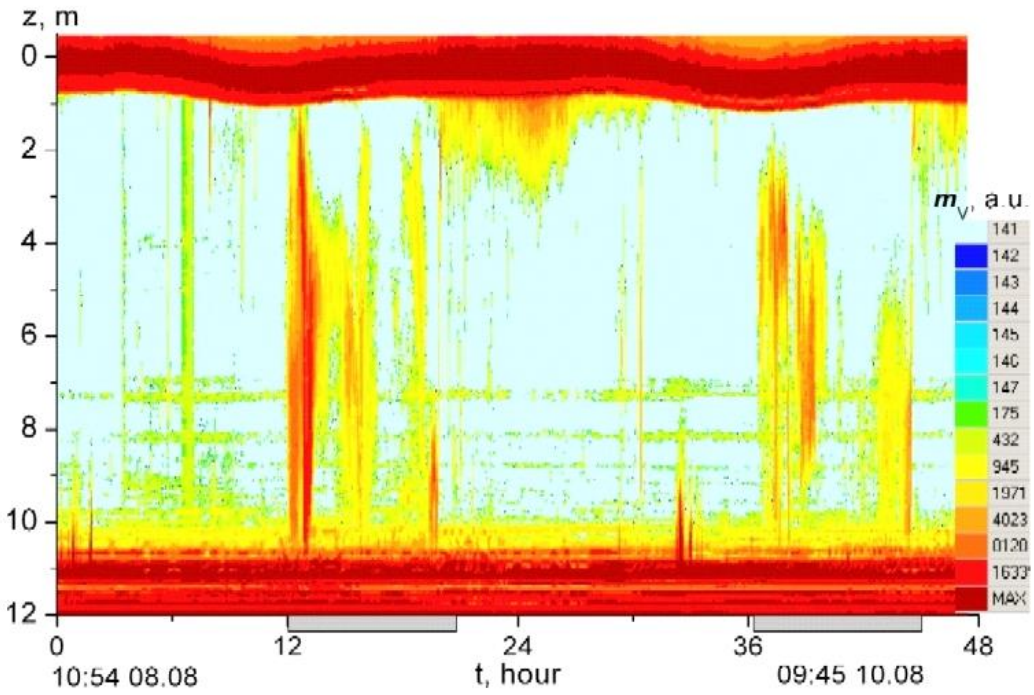

Fig. 4. Changes in the volume scattering coefficient of sound at a frequency of 138 kHz for two days from 10:54 on August 8 to 09:45 on August 10, 2017.

Sound scattering is often displayed as a layer strength and recorded in logarithmic form according to the formula $S_V = 10\lg < m_V >$, where $< m_V >= (1/h)\int_h m_V(z)dz$, at the same time, the dimension of m_V is taken in 1/m. Figure 5 shows the dependence of the average depth value on time in the entire water layer.

Preprints (www.preprints.org) | NOT PEER-REVIEWED | Posted: 4 May 2022 doi:10.20944/preprints202205.0013.v1

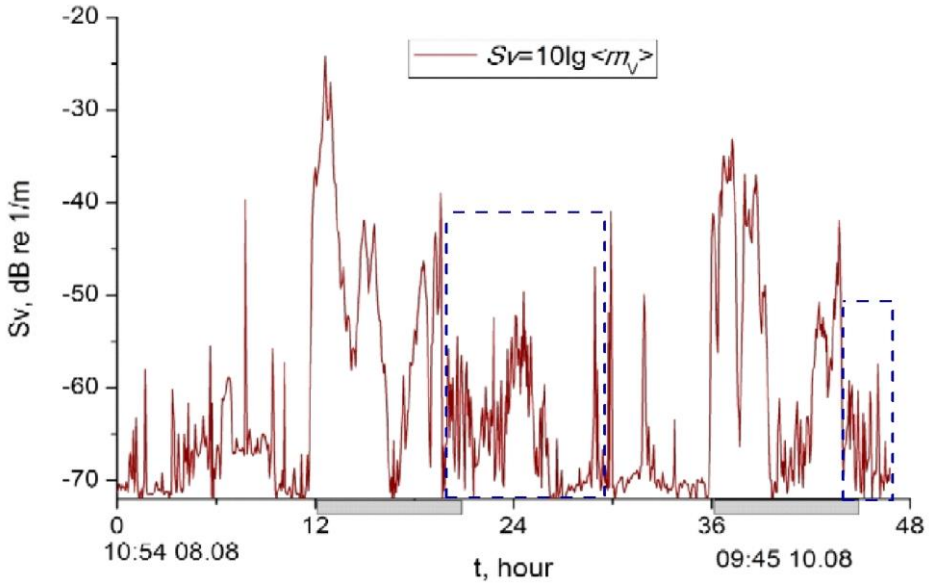

Fig. 5. Change in the average sound scattering coefficient SV for two days. The areas where the main contribution is made by bubbles are highlighted.

It can be seen from Fig. 5 that during the night period the strength of the S_V layer increases sharply, which is primarily due to diurnal migrations of plankton. The increased values in the daytime are associated with bubble clouds, the time intervals of which are highlighted with a dashed line in Fig. 5. Sound scattering on the shelf is largely of biological origin and is almost an order of magnitude higher at night compared to daytime values. In Fig. 6 presents a detailed picture of sound scattering at a frequency of 145 kHz on near-surface bubble clouds and simultaneous sound scattering on plankton communities involved in the dynamics of internal waves. At the top and right of the figure are horizontal and vertical profiles of the sound scattering coefficient mV along the lines shown in Fig. 6. A more detailed picture of the wave dynamics of plankton is presented in the upper inset. It can be seen that a powerful layer of bubbles is observed near the surface, extending to a depth of about 4-5 meters.

Preprints (www.preprints.org) | NOT PEER-REVIEWED | Posted: 4 May 2022 doi:10.20944/preprints202205.0013.v1

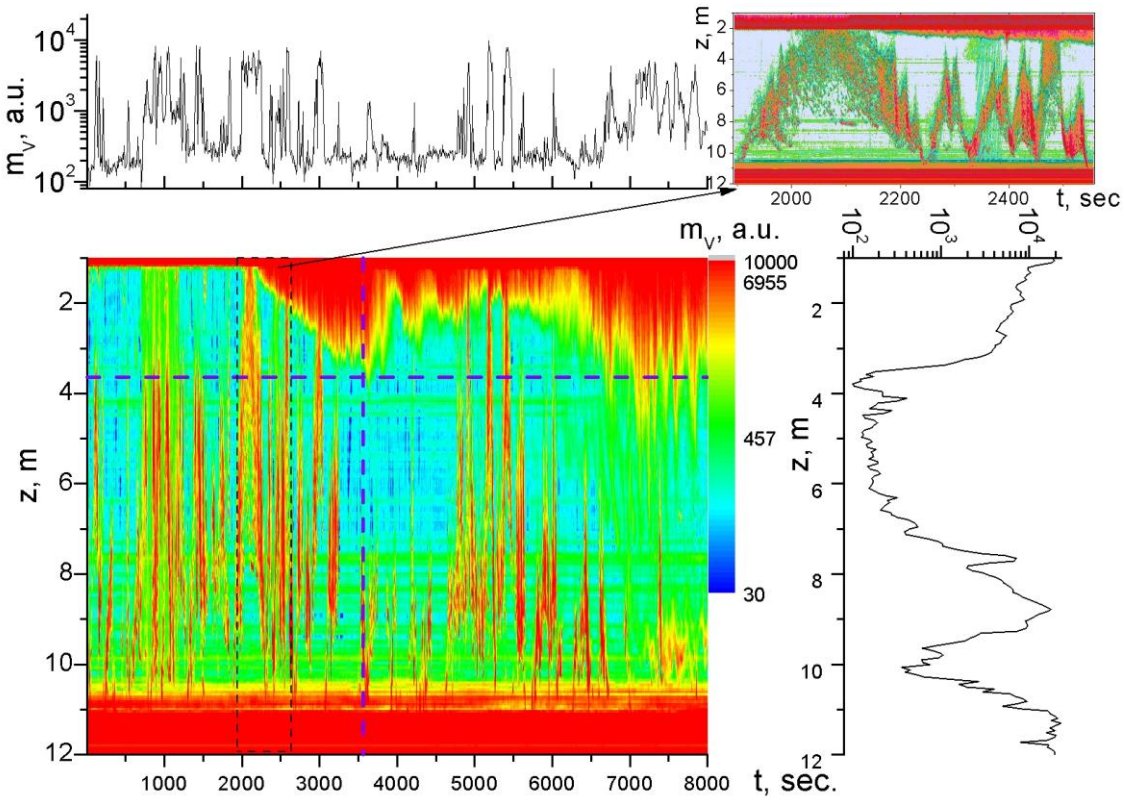

Fig. 6. Sound scattering on near-surface bubble clouds and simultaneous sound scattering on zooplankton.

Figure 7 shows the most typical results for various sound frequencies during 2 days of continuous recording of scattering on the shroud of bubbles involved in the water column by wind stresses.

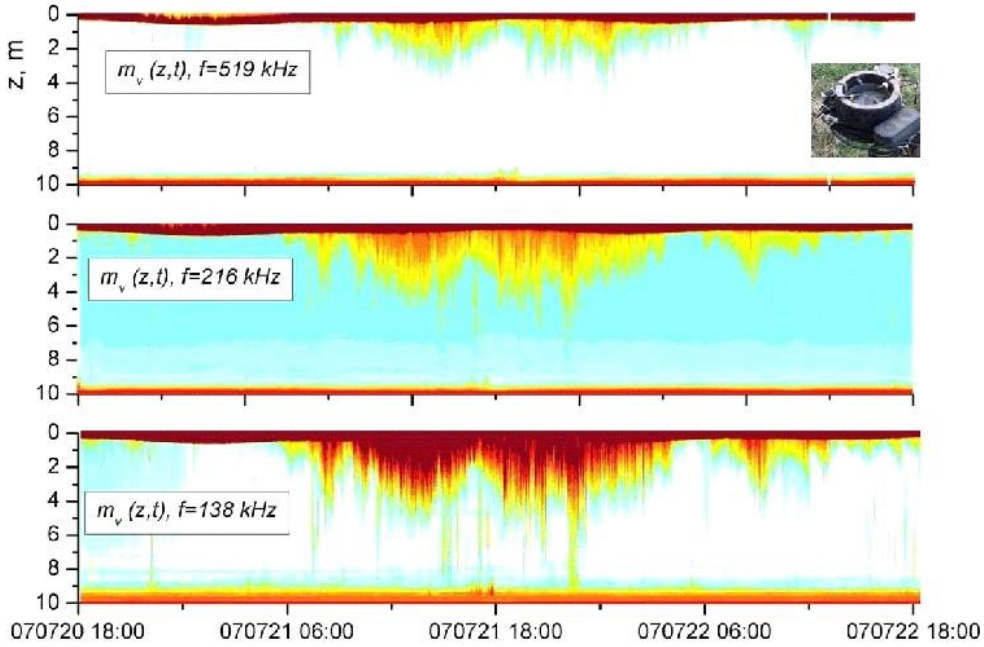

Fig. 7. Variations of the sound scattering coefficient at frequencies 138, 216 and 519 kHz caused by bubble clouds during 2 days.

.

Preprints (www.preprints.org) | NOT PEER-REVIEWED | Posted: 4 May 2022 doi:10.20944/preprints202205.0013.v1

Figure 8 shows a detailed recording of the sound backscattering signals from the bottom station at a frequency of 138 kHz. Variations of sound scattering caused by air bubbles involved in the sea water column to a depth of 5-7 meters are clearly visible.

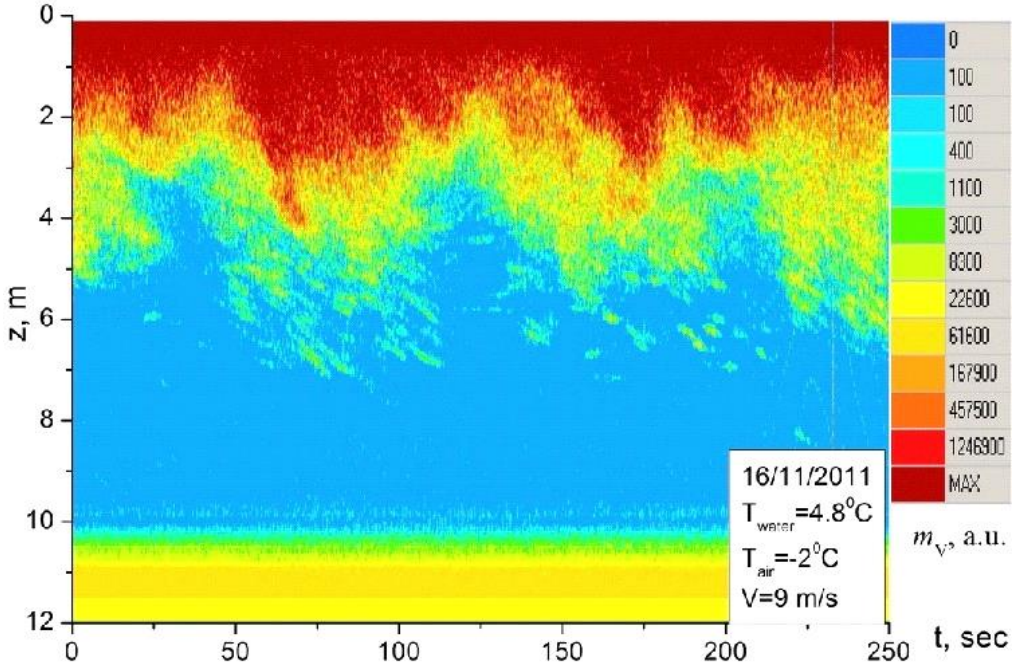

Fig. 8. Studies of sound scattering from the bottom station at a frequency of 138 kHz in order to study the near-surface layer of bubbles formed during the collapse of surface waves.

3.2. Bubble size distribution function

The obtained data on sound scattering using formulas (4) and (10) allow us to obtain bubble size distribution functions. Instead of the value $g(R)$ having dimension [cm^{-4}], the value $N(R)$ is often used It has dimension [m^{-3}mkm^{-1}], which is associated with the $g(R)$ relation $N(R) = 10^2 g(R)$. At a fixed frequency of 138 kHz, which corresponds to a resonant size of 23 microns, the value of $N(R)$ resonant bubbles is shown in Fig. 9 for different depths during the change of surface waves.

Preprints (www.preprints.org) | NOT PEER-REVIEWED | Posted: 4 May 2022 doi:10.20944/preprints202205.0013.v1

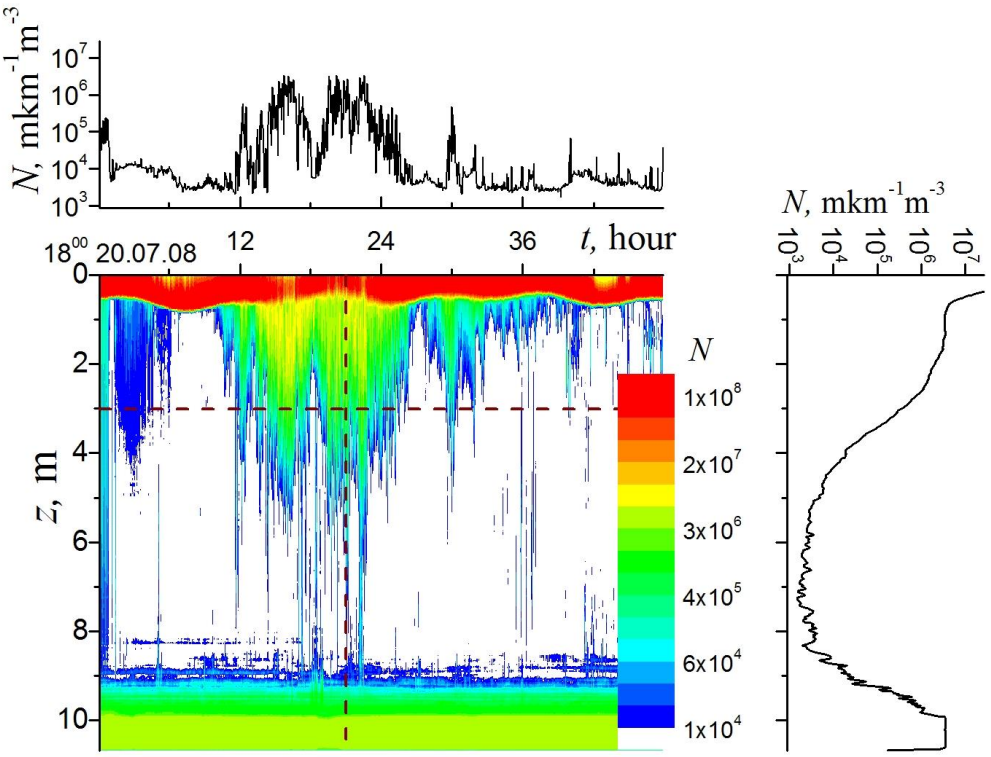

Fig. 9. Distribution of bubbles resonant at a frequency of 138 kHz in depth and its change over two days due to variations in wind speed (4 - 14 m/s) and sea waves: the upper figure is the change in time of the concentration of bubbles at a depth of 3 m, the figure on the right is the section $N(z)$ at the time 21 hours from the start of the experiment, indicated by a vertical line.

Experimental data on sound scattering in a wide frequency band using formula (10) allowed us to obtain bubble size distribution functions, which for different depths are shown in Fig. 10 for different sea conditions: before a storm, during a storm and after a storm.

Preprints (www.preprints.org) | NOT PEER-REVIEWED | Posted: 4 May 2022 doi:10.20944/preprints202205.0013.v1

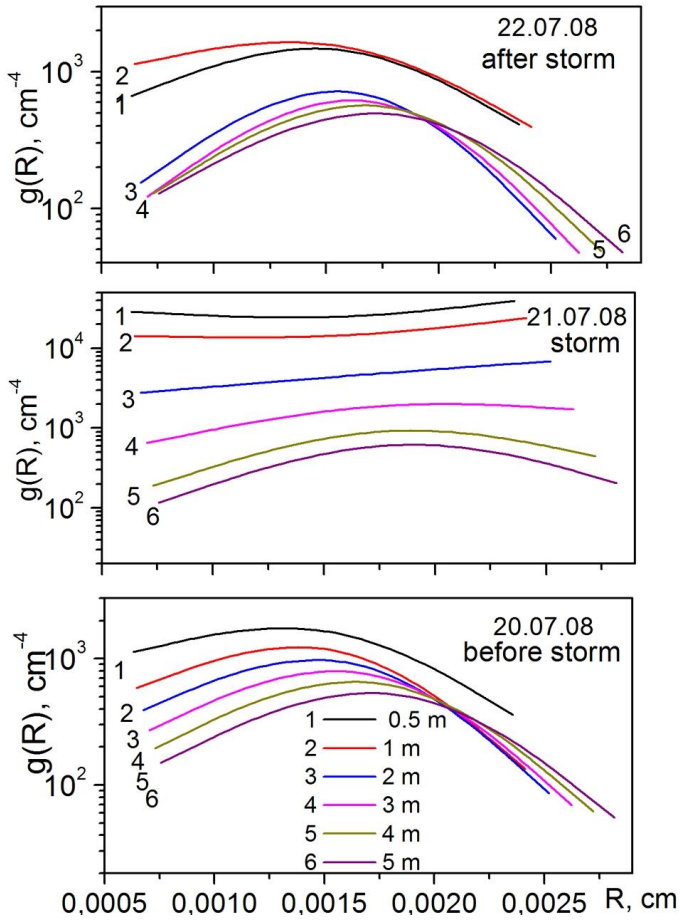

Fig. 10. Bubble size distribution function $g(R)$ at different depths during different time periods of storm development.

It can be seen from Fig. 10 that during periods without a storm, the maximum of the function $g(R,z)$ is observed, which is located at $R_p > 10$ microns, while the value R_p depends on the depth. At $R > R_p$, there is a power dependence of the bubble size distribution function with an exponential decline with depth. Taking into account the decline of the function $g(R)$ at small R, the presence of a maximum at $R = R_p$ and limiting the spectrum from above to the maximum bubble size R_m allows us to represent the bubble size distribution in an analytical form by the following formula [14]:

$$g(R,z) = A_g R^{-n(z)} \exp\left[-m\left(\frac{R_p}{R} + \frac{R}{R_m}\right)\right] e^{-z/L}, \qquad (19)$$

where $L \sim (2 \div 4)\cdot 10^{-3} U_{10}^{2,5}$ (here L is given in meters, the wind speed U_{10} at an altitude of 10 m is given in m/s), the indicator m depends on the state of the sea, $m = 1 \div 3$, for moderate and calm waves $m \approx 1$. The advantage of such a record $g(R)$ is the practicality and speed of calculations of various parameters of the environment. It is also important that the exponent n~3.3 and the critical dimensions R_p, R_m are natural parameters that follow from the Garrett–Lee–Farmer theory (GLF) [22]. Measurements of $g(R)$ on a large factual material under similar conditions of moderate sea conditions give values in the interval $n \approx 3.3 \div 3.8$ [3-6, 17, 18], which is close enough to the estimate of n~3.3 obtained for the inertial interval between the sizes R_p, R_m, following from the theory of GLF [22].

Preprints (www.preprints.org) | NOT PEER-REVIEWED | Posted: 4 May 2022 doi:10.20944/preprints202205.0013.v1

So, it is shown that a weakly perturbed structure is characterized by the presence of $g(R)$ with a maximum, the position of which varies depending on the depth. A completely different picture is observed during a storm - here a large number of both large and small bubbles are formed in the near-surface layers in the absence of a visible maximum, which, nevertheless, is available for bubbles located in the water column with depths greater than 3 meters.

3.3. Estimates of gas content and sound absorption from experimental data

The sound absorption coefficient was calculated on the basis of experimental data obtained by sound scattering on bubble structures according to the formula (18). Figure 11 shows, as a typical example, calculations for sound absorption at a frequency of 145 kHz in the near-surface layer of bubbles at wind speeds from 9 to 13 m/s for about a day.

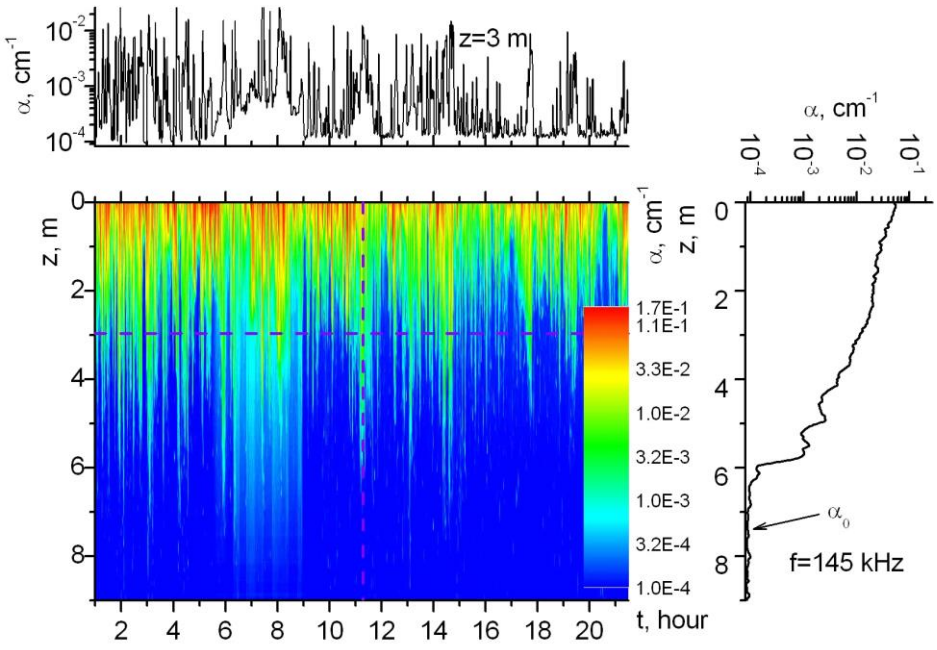

Fig. 11. Time changes in the sound absorption coefficient at a frequency of 145 kHz in the near-surface layer of bubbles at wind speeds from 9 to 13 m/s.

Figure 11 shows a significant excess absorption of sound in the bubble layer. Near the sea surface, sound absorption is 100 times higher than sound absorption in clear water $\alpha_0 \approx 10^{-6}$ 1/m. At great depths, sound absorption tends to the value of sound absorption in clear water. There is a significant variability in the thickness of the layer by the sound absorption coefficient, varying from 7 m to 1.5-2 m.

Important for practical applications is information about the gas content and structure of bubble clouds arising from the collapse of surface waves. Using the data for sound scattering, it is possible to calculate the bubble size distribution function, and then, as well as for sound absorption, shown above in Figure 11, to obtain data on the change in time of the average volume concentration of the gas $x = (4\pi/3)\int_{\{R\}} g(R)R^3 dR$ contained in the bubbles in the entire thickness of the seawater layer. We regularly carried out measurements of near-surface sound

Preprints (www.preprints.org) | NOT PEER-REVIEWED | Posted: 4 May 2022 doi:10.20944/preprints202205.0013.v1

scattering associated with bubble structures. A typical change in time of the average volume concentration of gas contained in bubbles in the entire thickness of the sea water layer at a wind speed varying from 9 to 13 m/ s is shown in Fig. 12 a. The spectrum of the gas concentration function is shown in Fig. 12 b. It can be seen that the concentration of bubbles is quite large, while it should be noted a significant variability in time of the average concentration of gas contained in the bubbles, which is due to the periodic collapse of wind surface waves and the formation of bubble clouds that reach a depth of 7-8 m. Characteristic spectral peaks are visible, corresponding to periods of wind amplification above the sea surface and leading to abnormal sound absorption with a change in the $g(R)$ function, the details of which are visible in Fig. 11.

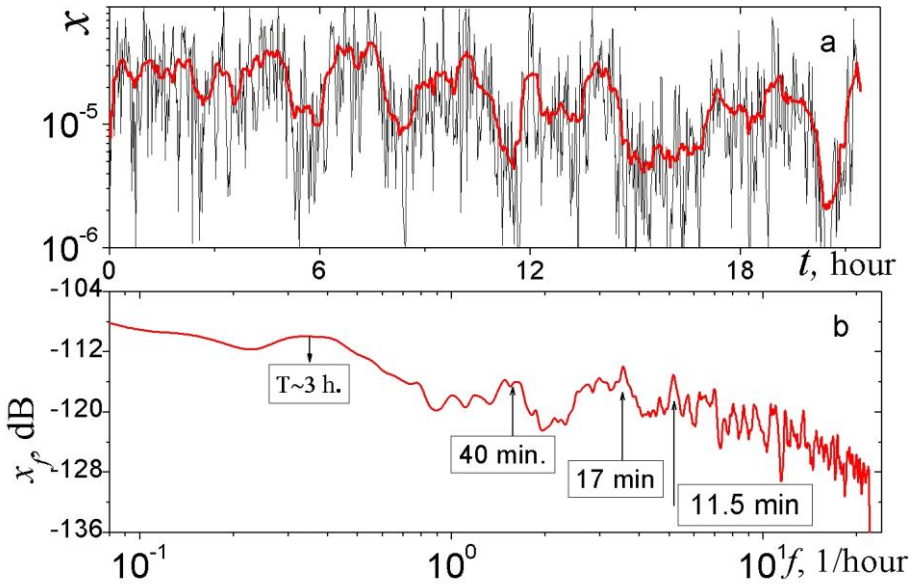

Fig. 12. Variability in time of the average volume concentration of gas $x(t)$ contained in bubbles (a) and the spectrum of the gas concentration function (b) in the presence of bubble clouds formed by the collapse of wind waves.

3.4. On the propagation of sound in the presence of near-surface bubble clouds

To study the influence of the near-surface layer of bubbles on the propagation of sound, numerical modeling was carried out for a shallow sea using the approximation of normal modes. For ease of analysis, a model of the simplest horizontally homogeneous, bubble–free isoscale underwater sound channel with absolutely reflective boundaries was chosen (the upper boundary is soft, the lower one is hard). The sound pressure is represented as the sum of normal modes. The additional attenuation caused by the presence of a bubble layer is described by the imaginary part of the eigenvalues of the modes. Calculations of the sound field were performed using the KRAKENC program [23] for interacting modes. The thickness of the bubble layer was chosen equal to 7 meters. The emitter with a frequency of f = 1 kHz was located at a depth of 10 meters at a sea depth of 42 m.

Figure 13 shows a 2D image of the acoustic field for different concentrations of bubbles in the near-surface layer. The calculations in Fig. 13 show a strong change in the structure of the acoustic field when the concentration of bubbles exceeds 10^{-7}. For this concentration of bubbles, the acoustic field in the bubble layer near the surface attenuates at a distance of about 400 m. The result is particularly impressive for a concentration of 10^{-6}. Here, the field near the surface fades

Preprints (www.preprints.org) | NOT PEER-REVIEWED | Posted: 4 May 2022 doi:10.20944/preprints202205.0013.v1

already at a distance of about 100 m. At the same time, the overall structure of the acoustic field in the thickness of the waveguide changes dramatically.

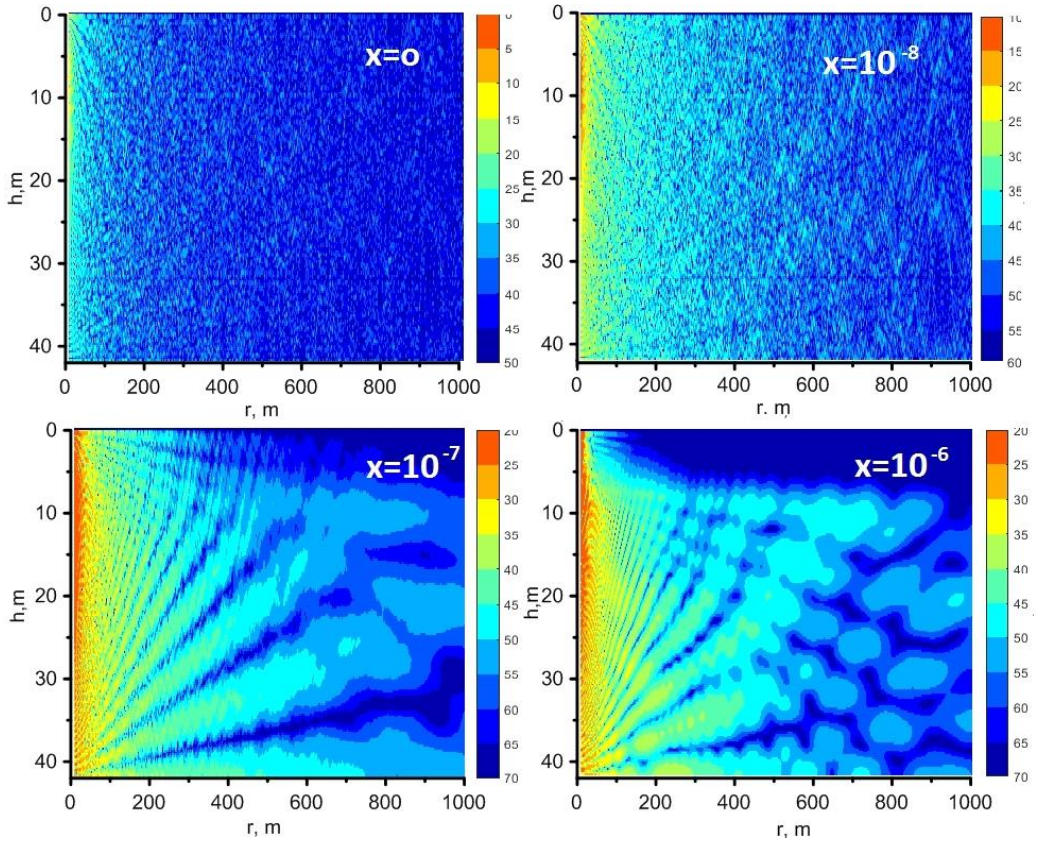

Fig. 13. Acoustic field of a source with a frequency f = 1 kHz at a depth of 10 meters in a channel with a near-surface layer of bubbles 7 m thick at different concentrations of bubbles: x = 0, $x = 10^{-8}$, $x = 10^{-7}$, $x = 10^{-6}$.

Figure 14 shows the dependences on the distance of the acoustic field pressure $|p(r,z)|$ at different concentrations of bubbles. Thick lines show the average depth pressure of the acoustic field. Figure 14 shows a strong dependence of the field decline on the distance at different depths. But at large distances, the nature of the exponential decline of the field turns out to be close for various depths, including the average field. At large distances, the main contribution to the energy of the field is made only by those components that do not interact strongly with the bubble layer, and therefore the sound absorption coefficient decreases sharply and approaches the value of the absorption coefficient in water without bubbles.

Preprints (www.preprints.org) | NOT PEER-REVIEWED | Posted: 4 May 2022 doi:10.20944/preprints202205.0013.v1

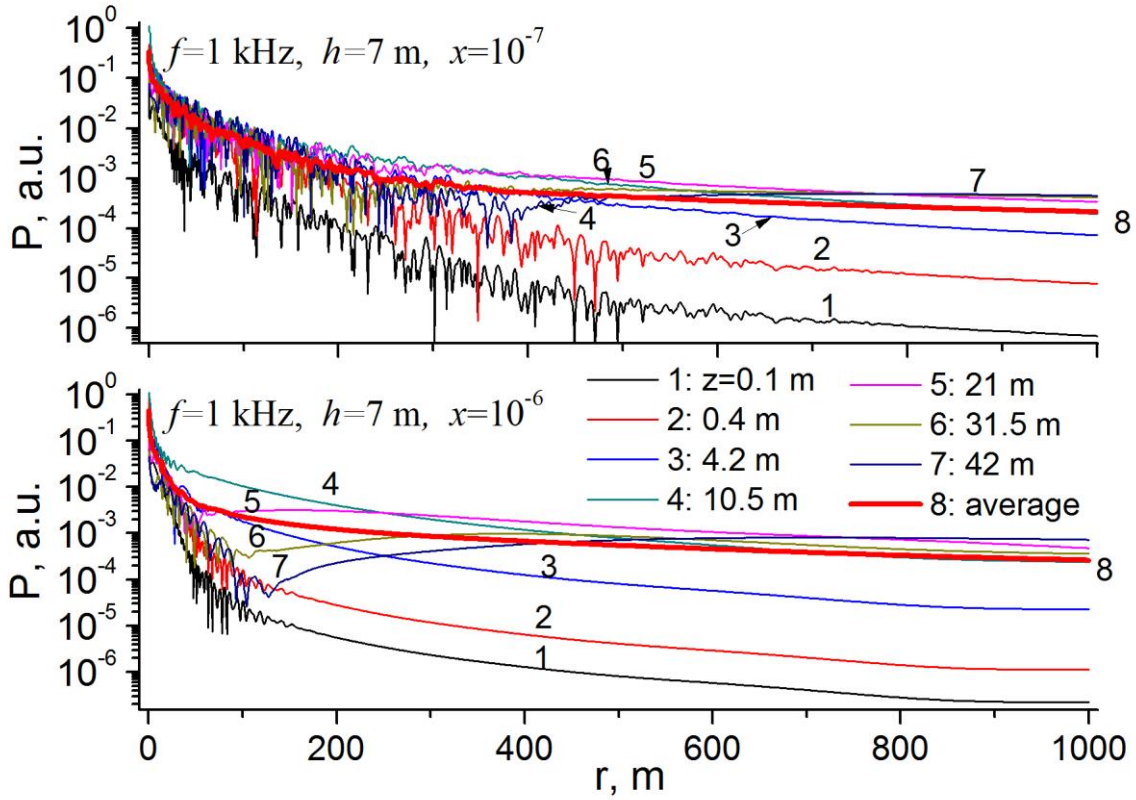

Fig. 14. Dependences on the acoustic field pressure distance $|p(r,z)|$ at different bubble concentrations and constant layer thickness h = 7 m. Thick lines show the average depth pressure of the acoustic field $P(r) = <|p(r,z)|>_z$.

As a characteristic of the decline of the acoustic field with distance, we can take an expression for the average depth of the field of the form $P(r) = <|p(r,z)|>_z = (1/h)\int_0^h |p(r,z)|dz$, where h is the depth of the channel. Then $P(r)$ it can be written in the form $P(r) = A\exp(-\alpha r)/\sqrt{r}$ according to which the attenuation coefficient of the sound can be calculated. The results of calculating the coefficients α show the following values α: α =1.5*10^{-5} 1/m at x=0; α =9.5*10^{-4} 1/m at x=10^{-8}; α =7.4*10^{-3} 1/m at x=10^{-6}. For comparison, the absorption coefficient of a plane sound wave α_b at a frequency of 1 kHz for the case of a homogeneous veil of bubbles in seawater has the following values: α_b =1.5*10^{-5} 1/m at x=0; α_b=3.5*10^{-3} 1/m at x=10^{-8}; α_b=3.2*10^{-1} 1/m at x=10^{-6}.

Figures 15 and 16 show the dependences on the acoustic field pressure distance at different frequencies $|p(r;f)|$ without a bubble layer and in the presence of a bubble layer. It can be seen that the presence of even a relatively small concentration of bubbles x = 10^{-7} in the layer leads to a significant absorption of sound along the propagation path. At the same time, a significantly stronger frequency dependence is observed compared to the absence of a bubble layer.

Preprints (www.preprints.org) | NOT PEER-REVIEWED | Posted: 4 May 2022 doi:10.20944/preprints202205.0013.v1

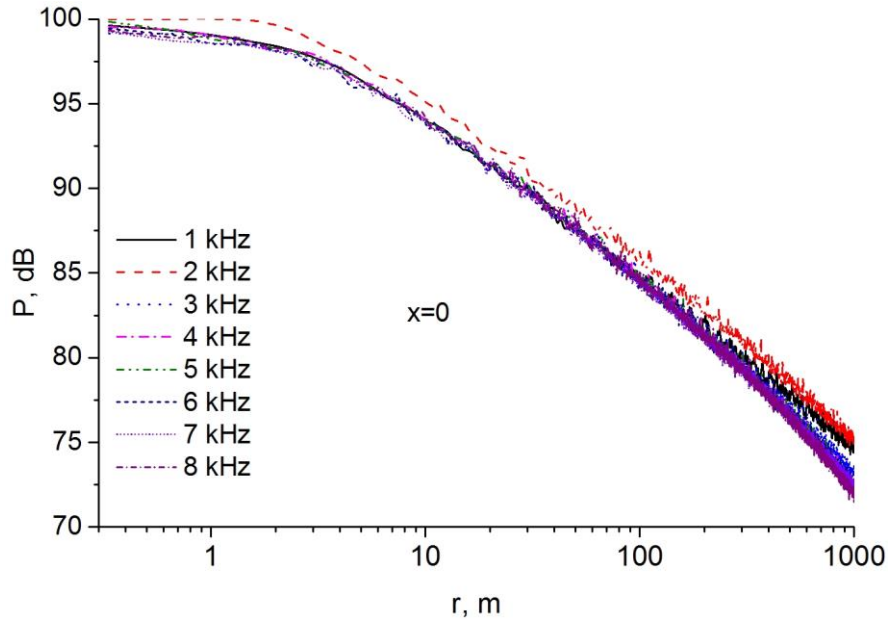

Fig. 15. Dependences on the acoustic field pressure distance at different frequencies $|p(r;f)|$ without bubble layer

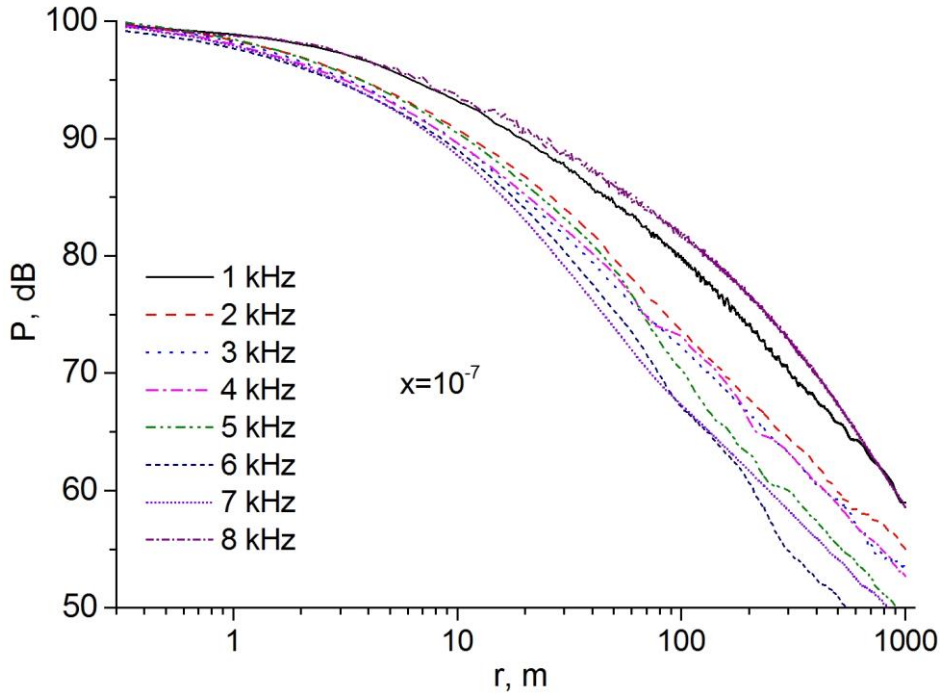

Fig. 16. Dependences $|p(r;f)|$ at bubble concentrations $x=10^{-7}$ and constant layer thickness h=7 m.

4. Discussion

The above results were obtained in a shallow sea, which is characterized by strong variability of the near-surface layer, as well as the simultaneous content of various micro-heterogeneities. Figures 4-6 show typical results of sound scattering, which show the presence of various objects - bubble clouds and plankton. The contributions to the scattered signals from them often

Preprints (www.preprints.org) | NOT PEER-REVIEWED | Posted: 4 May 2022 doi:10.20944/preprints202205.0013.v1

intersected, and with the standard procedure for processing acoustic data, it is extremely difficult and often impossible to separate these contributions.

To separate sound scattering on bubbles from scattering on plankton, we used the method of unsteady scattering of pulses of different durations with different frequencies [17, 18], which was previously used to study the spectral distribution of bubbles in the near-surface layers of the deep sea. Figure 7 shows a typical application of pulses with different frequencies to obtain information about the structure of bubble clouds and their dynamics for several days. Figure 8, representing the recording of backscattering signals for four minutes, illustrates in detail the variability of the near-surface layer of bubbles formed during the collapse of surface waves and reaching a depth of about 7 m. It should be noted that the data in Fig.8 refer to the autumn-winter period, when the air temperature becomes significantly lower than the water temperature. It is possible that it is under these conditions that facilitated conditions are created for transporting cooled layers of water with bubbles into the sea, despite the rather small wind speed shown in the inset Fig.8. It should be noted that in the experiments shown in Fig. 6 and Fig.8, a quasi-homogeneous near-surface layer of bubbles can be observed. The alternation of individual acts of collapse of surface waves in shallow sea conditions roughly coincides with similar ones in open deep sea conditions. It can be assumed that the reason for the overlap and formation of a quasi-homogeneous structure of bubble clouds in shallow sea conditions is the gradual pumping of gas during the collapse of waves. Such aeration of the near-surface layers creates an increased gas content in the water, which prevents the rapid dissolution of bubbles and, under certain conditions, maintains an equilibrium concentration of bubbles in the near-surface layers of the sea.

Experimental data on sound scattering made it possible to present the size distribution of bubbles in an analytical form using a semi-empirical formula (19). This formula is in many respects close to the known dependencies proposed in the literature [7, 11, 13, 14]. The advantage of formula (19) is the practicality and speed of calculating the acoustic characteristics of water with bubbles. Attention should be paid to the presence of a fitting parameter in formula (19) – the size R_p corresponding to the maximum of the function $g(R)$. This parameter is important for more accurate calculations. However, its magnitude has not yet been very clearly studied. So from Fig.10 it can be seen that in conditions of moderate wind and a weak layer of bubbles, the value R_p can be estimated at about 10 microns. However, even in conditions of strong wind, the distribution of bubbles in Fig.10 indicates a wider distribution in size and, in particular, indicates a shift of the maximum R_p towards values less than 10 microns. This issue requires further study.

The creation of a quasi-homogeneous layer can lead to important changes in the physical characteristics of the structure of the surface layer of the sea. Particular attention should be paid to the variability of acoustic characteristics – the dispersion of sound velocity and sound absorption. In the case of a quasi-homogeneous layer, their variability will be determined mainly not by individual acts of collapse of surface waves, but by the very average structure of such a layer, which, presumably with a strong wind, can be located under the sea surface at considerable distances. Examples of data processing for studying the variability of the sound absorption coefficient and the volume content of gas in bubbles, shown in Fig. 11 and Fig.12, show the presence of a quasi-homogeneous background near-surface layer. The periods of its variability are much longer than the typical periods of collapse of surface waves.

The modeling of sound propagation in the conditions of such a quasi-homogeneous layer, undertaken in our work, shows that its influence is very significant. It leads both to a change in the laws of the average decay of the sound field along the sound propagation path, and to a change in the shallow spatial structure of the field. It seems important to us to pay attention to the fact that at long distances, despite the presence of a bubble layer, an additional change in the

 doi:10.20944/preprints202205.0013.v1

amplitude of the field stops due to the exponential decline caused by the presence of bubbles. The mechanism of such an impact seems to us as follows. The influence of the near-surface layer of bubbles consists in an additional decrease in the field at moderate distances caused by the attenuation of part of the sound energy propagating in the bubble layer. In the future, this energy is completely absorbed, which eventually leads to the absence of the contribution of the bubble layer in the exponential law – only exponential attenuation due to dissipative processes in seawater remains. Nevertheless, the presence of dissipation in the near–surface layer of bubbles can lead to a significant restructuring of the structure of the acoustic field, as demonstrated in Figures 13-15.

Conclusion

The study of the structure of the upper layer of the sea saturated with gas bubbles, as well as their relationship with the acoustic characteristics of bubble clouds formed by the collapse of surface waves in a strong wind. Experimental studies were carried out in the shallow sea using the method of non-stationary acoustic spectroscopy, the discussion of which is presented in the article. Data on the size distribution of bubbles at various depths have been obtained, which can be described by a power function with exponential decline at small bubble sizes of the order of 10 microns. Estimates of the gas content in bubble clouds under various sea conditions, including storm conditions, have been carried out. In order to study the effect of bubbles on the acoustic characteristics of the upper layer of the sea, theoretical estimates of the dependences of the absorption coefficient and the dispersion of the sound velocity on the concentration of bubbles were obtained within the framework of a homogeneous model. It was found that there is a significant excess absorption of sound in bubble clouds, which is hundreds of times higher near the sea surface than the absorption of sound in clear water. It is shown that using unsteady sound scattering, it is possible to identify the detailed structure of near-surface bubble clouds, their dynamics and determine the variability of the acoustic characteristics of the near-surface layer under various sea conditions, including the processes of collapse of wind surface waves in a developed storm. It is shown that when the wind increases in a shallow sea, a quasi-homogeneous near-surface layer of bubbles is observed. Modeling of sound propagation in the presence of a quasi-homogeneous bubble layer shows that it leads both to a change in the laws of the average decay of the sound field along the sound propagation path and to a change in the shallow spatial structure of the field.

Funding:

The work was carried out within the framework of the POI FEB RAS project No. 0211-2021-0002.

Acknowledgments:

The authors are grateful to I.V. Korskov for technical support during the experiments and S.N. Sosedko for assistance in processing experimental data.

Author's contribution:

Conceptualization, VB and LB; Methodology, VB; Software, LB, AB; Validation, VB, AB and LB; Formal Analysis, VB; Investigation, VB, AB and LB; Resources, VB; Data Curation, VB,

AB; Writing – Original Draft Preparation, VB.; Writing – Review & Editing, VB; Visualization, VB, AB and LB; Supervision, VB; Project Administration, VB; Funding Acquisition, VB.

VB – V.A. Bulanov, LB – L.K. Bugaeva, AV – A.V. Storozhenko

References

1. Brekhovskikh L.M., Lysanov Yu.P. Fundamentals of ocean acoustics. Berlin, N.Y.: Springer, 1982, 250 p.
2. H. Medwin, “Acoustical determination of bubble size spectra” // J. Acoust. Soc. Am. 1977. Vol. 62, pp. 1041-1044.
3. H. Medwin, “In situ acoustic measurements of microbubbles at sea”, J. Geophys. Res , 82(6), 971-976 (1977).
4. S.A. Thorpe, “On the clouds of bubbles formed by breaking wind-waves in deep water, and their role in air-sea gas transfer”, Phil. Tran. R. Soc. Lond. A, 304, 155-210 (1982).
5. Thorpe S.A. Measurements with an automatically recording inverted echo sounder; ARIES and the bubble clouds // J.Phys.Oceanography. 1986. V. 16. P. 1462-1478.
6. S. Vagle, D. Farmer, "The measurement of bubble-size distributions by acoustical backscatter", Journ. of Atmospheric and Oceanic Technology, 1992. Vol. 9, pp.630-664.
7. Wu, J. Bubbles in the near-surface ocean: Their various structures. J. Phys. Oceanogr. 1994, 24, 1955–1965.
8. Lamarre, E.; Melville,W.K. Sound speed measurements near the ocean surface. J. Acoust. Soc. Am. 1994, 96, 3605–3616.
9. E. L. Andreas, E. C. Monahan, “The role of whitecap bubbles in air-sea heat and moisture exchange”, J. Phys. Oceanogr., 2000, Vol. 30, pp.433-441.
10. Lei Han, YeLi Yuan. Bubble size distribution in surface wave breaking entraining process. // Science in China Series D: Earth Sciences. 2007. Vol. 50, No 11, pp.1754-1760
11. S. Vagle, C. McNeil, N. Steiner. Upper ocean bubble measurements from the NE Pacific and estimates of their role in air-sea gas transfer of the weakly soluble gases nitrogen and oxygen// J. Geophys. Res., 2010, Vol. 115, C12054, doi:10.1029/2009JC005990.
12. B. Baschek, D. M. Farmer. Gas Bubbles as Oceanographic Tracers. Journal of Atmospheric and Oceanic Technology . 2010. Vol.27. No 1, pp.241-245
13. H. Czerski, G. B. Deane. The effect of coupling on bubble fragmentation acoustics // J. Acoust. Soc. Am. 2011. Vol. 129, No 1, p.74
14. Deane G.B., Preisig J.C., Lavery A.C. The suspension of large bubbles near the seasurface by turbulence and their role in absorbing forward-scattered sound // IEEE Journ.of Oceanic Eng., 2013. V. 38, NO. 4, P.632-641; DOI: 10.1109/JOE.2013.2257573
15. Ainslie, M. A., 2005, Effect of wind-generated bubbles on fixed range acoustic attenuation in shallow water at 1-4 kHz, J. Acoust. Soc. Am., Vol. 118(6), pp. 3513-3523.
16. Liu, R.; Li, Z. The Effects of Bubble Scattering on Sound Propagation in ShallowWater. J. Mar. Sci. Eng. 2021, 9, 1441. https://doi.org/10.3390/jmse9121441
17. Akulichev V.A., Bulanov V.A., Klenin S.A. Acoustic sensing of gas bubbles in the ocean medium // Soviet Physics. Acoustics. 1986. V. 32. № 3. P. 177-180.

18. V.A. Akulichev, V.A. Bulanov. Measurements of bubbles in sea water by nonstationary sound scattering // J. Acoust. Soc. Am. 2011. Vol.130, No5, pt.2, pp.3438-3449
19. Naugolnykh K.A., Ostrovsky L.A. Nonlinear Wave Processes in Acoustics, Cambridge: University Press, 1998. 298 p.
20. V.A. Akulichev, V.A. Bulanov. Anomalies in Acoustic Parameters of Polydisperse Liquids with Gas and Vapor Bubbles Doklady Earth Sciences, 2013, Vol. 448, Part 1, pp. 92–96. DOI: 10.1134/S1028334X13010091
21. Bulanov V.A., Korskov I.V., Sosedko S.N., Storozhenko A.V. A multifrequency acoustic sounding system for studying the acoustic characteristics of the upper layer of the sea Instruments and Experimental Techniques. 2020. T. 63. № 3. C. 410-415.
22. Garrett C., Li M., Farmer D. The Connection between Bubble Size Spectra and Energy Dissipation Rates in the Upper Ocean // J. Phys. Ocean. 2000. V. 30. No 9. P. 2163-2171.
23. Porter, M. B., Reiss, E. L., 1985, A numerical method for bottom interacting ocean acoustic normal modes, J. Acoust. Soc. Am., Vol. 77(5), pp. 1760-1767; Code, online at http://oalib.hlsresearch.com/Modes/, accessed on September 3, 2019.